

Fusion of conventional ultrasound imaging and acousto-optical sensing (AOS) using a
standard pulsed ultrasound scanner.

5 Emmanuel Bossy*, Lei Sui, Todd W.Murray and Ronald A. Roy

Department of Aerospace and Mechanical Engineering

Boston University

110 Cummington Street

Boston, MA 02215

10

Corresponding author: email Emmanuel.Bossy@espci.fr

Fusion of conventional ultrasound imaging and acousto-optical sensing
(AOS) using a standard pulsed-ultrasound scanner.

5 ABSTRACT

Acousto-optical sensing (AOS) is a dual-wave sensing technique based on the ultrasound modulation of diffuse light in a turbid medium. We experimentally demonstrate the feasibility of combining AOS and conventional ultrasound imaging by using a
10 commercially available pulsed-ultrasound scanner coupled with a photorefractive crystal-based optical interferometry system. Optically absorbing targets embedded in highly diffusive phantoms ($\mu_s' = 10 \text{ cm}^{-1}$) are imaged through a thickness of 27 mm with millimeter resolution. The AO images are intrinsically co-registered with the ultrasound images.

A number of techniques aimed at imaging the optical properties of biological tissue have been introduced recently.¹ Subsurface optical imaging of biological tissue is complicated by the fact that the media is highly scattering, making it difficult to achieve good spatial resolution at large imaging depths. In this context, acousto-optical sensing (AOS) shows promise, for this technique derives from the combination of light and ultrasound.² Briefly, ultrasound is used to phase modulate or "tag" diffuse light, and the detection of the modulated light yields spatially resolved optical information. The spatial resolution of this imaging technique is dictated by the ultrasound distribution. To date, several variations of this technique have been introduced, based on different optical detection schemes, different types of ultrasonic waveforms and different signal processing techniques.²⁻⁷

Pulsed ultrasound is a well established clinical imaging technique, yielding information on the bulk mechanical and interfacial properties of the medium. AOS has the potential to augment the existing technology by generating additional information regarding spatially dependent optical properties. The idea of combining information from ultrasound and AOS was first proposed by Leveque-Fort *et al.*⁸, who employed CW ultrasound to generate AO signals⁹. While CW ultrasound supports narrow bandwidth optical detection systems, and subsequent enhancement in signal to noise ratio (SNR), it affords limited axial resolution and can produce deleterious thermal effects on biological tissue. On the other hand, short-duration ultrasonic pulses are desirable provided that SNR limitations can be overcome. Short-pulse ultrasound yields axial resolution that is equal to the spatial pulse length, while employing low time-averaged acoustic power levels. Using a succession of phased-synchronized ultrasound pulses, Lev *et al.* were able to map the photon density *in vitro* using a tissue phantom.⁶ More recently, a photorefractive crystal (PRC) based interferometry system has been introduced by Murray *et al.*¹⁰, allowing for the detection of AO signals within highly diffuse media using pulsed ultrasound. This technique is further shown to be capable of imaging the optical inhomogeneity along the ultrasonic axis using time-averaged AO signals.¹¹ Based on this approach, this letter reports the feasibility of simultaneously imaging both acoustic and AO properties using pulsed ultrasound generated by a clinical US scanner.

The experimental setup is given in Figure 1. It combines a PRC-based optical detection system¹⁰ with a commercially available, PC-based, diagnostic ultrasound scanner (AN2300, Analogic, Peabody, MA, USA). An 80 mW frequency-doubled Nd:YAG laser source is split into signal and reference beams. The reference beam is directed around the test tank and sent to the PRC. The signal beam is sent through a 10x beam expander along the Y-axis to the submerged tissue-mimicking phantom, and light scattered from the phantom is collected by a lens and directed into the PRC. The PRC is BSO crystal with dimensions 5x5x7 mm³ (X, Z, Y). A 4 kHz high voltage field (10⁵ V/m) is applied to the crystal to enhance the two-wave mixing process. The signal beam and diffracted reference beam exiting the crystal are collected by an avalanche photodiode (APD) with a 10-mm diameter active aperture. The signal from the APD is sent to the preamplifier (x10), low-pass filtered (<500 kHz), and digitized by the oscilloscope.

A commercially available ultrasound probe (192-element linear array, type 8802, B&K Medical, Herlev, Denmark) is excited by the AN2300 and projects 5 MHz ultrasonic pulses along the Z-axis to generate both ultrasound and AO images in the ZX-plane. The diffusive tissue phantoms consist of a transparent polyacrylamide gel seeded with 0.4- μ m diameter polystyrene microspheres to obtain a reduced scattering coefficient $\mu_s' \approx 10 \text{ cm}^{-1}$. The phantoms dimensions are 40x40x27 mm³ (X,Z,Y). During the manufacturing process, targets (2x2x8 mm³ or 3x3x8 mm³, along directions X, Z and Y) were embedded in the phantoms using dedicated molds. The targets are made of the same material as the whole phantom, with India ink added to increase the optical absorption coefficient while minimally altering the acoustical properties.

The operation of the PRC-based optical detection system with pulsed ultrasound has been described elsewhere^{10, 11}. For sake of clarity, we briefly discuss the origin and nature of the detected AO signals. Without ultrasound, the signal and reference beams interfere at the PRC, and the intensity grating is recorded in the PRC as an index grating through the photorefractive effect. The reference beam diffracts from the grating into the signal beam direction with a phase front matched to the signal beam. The signal and diffracted reference beams are in-phase and interfere constructively at the APD. When an ultrasound pulse is sent through the diffusive medium, part of the scattered signal beam is phase modulated at the location of the traveling ultrasound pulse. Assuming that the

duration of the AO interaction remains short compared to the response time of the crystal, the index grating in the PRC remains stationary, and the diffracted reference beam is no longer in phase with the transmitted signal beam. In this case As a result, the DC output at the APD is decreased during the AO interaction^{10, 11}. Therefore, the time-domain signal output at the APD is expected to reflect the distribution of detectable modulated photons along the ultrasound path.

To ultrasonically scan the XZ-plane, different groups of elements on the probe are successively activated and fired in concentric directions, with a fixed focal length (50 mm). Along the direction of ultrasonic propagation, time is converted to space using an assumed sound speed (1.5 mm/_s for our water-matched phantoms). To display grayscale images (B-mode image), the ultrasound scanner demodulates the received ultrasound echo train associated with a given scan line and converts the signal envelope function to grayscale. Because the envelop of an AO signal in the time-domain is expected to correlate directly with the photon distribution along the ultrasound path, AO images were built in the exact same manner, and superimposed on top of the B-mode images using a color-scale. As a consequence, B-mode and AO images were automatically co-registered. Whereas a single ultrasonic shot can be used to build one B-mode line, the low SNR requires that high pressure levels, longer pulses, and time-averaging be used to detect AO signals. Six-cycle-long, 5 MHz sine bursts (spatial length of about 1.2 mm) were used to generate the AO signals. The spatial peak, temporal peak (SPTP) excursion of the sine bursts was typically 1 MPa peak negative and 6 MPa peak positive. The pulse repetition frequency was about 3.3 kHz and each AO signal was coherently averaged 20,000 times, yielding a SNR of approximately 65:1.

Figure 2(a) shows the B-Mode image (left) and superimposed AO image (right) obtained from a phantom with a 2x2x8 mm³ absorber. The parallel horizontal lines that demarcate the proximal and distal interfaces of the target are due to imperfect bonding of the target and phantom materials during the manufacturing process. A typical AO signal obtained for an ultrasound path through the absorber is plotted on Fig. 2(b). The AO image has a field of view given by the circular region seen on Fig. 2(a), typically 20 mm in diameter. This distribution of detected modulated light is limited by the light distribution itself, but may also be limited by the aperture of the light collecting system.

Here, the phantom was positioned so that the absorber is located at the center of the light distribution and at the ultrasound focus, in order to optimize SNR and resolution. Both the lateral (X) and axial (Z) dimensions on the AO image visually agree with the actual dimension of the absorber (2 mm x 2mm).

5 Figure 3 further illustrates the enhanced axial resolution achieved when using pulsed ultrasound. Two absorbing targets were embedded along the Z axis, centered in the light distribution. As seen from the AO image on Fig. 3(a) and AO signal on Fig. 3(b), the two targets are clearly resolved along the propagation axis.

10 To further illustrate the ability of this technique to supplement conventional B-Mode imaging, a phantom was made with two embedded targets, one with India ink and the other without. The two targets appear identical in the B-Mode image (Fig. 4(a), left). On the other hand, the AO image (Fig. 4(a), right) leaves no doubt as to the differing absorbing nature of each target. In a clinical context, this suggests the ability to distinguish between optically distinct clinical features that would otherwise appear
15 identical on a conventional ultrasound image. These experimental results reported herein demonstrate that B-mode and AO sensing can be simultaneously implemented using a commercially available ultrasound scanner, yielding both acoustical and optical contrast information in the form of two automatically co-registered images. A standard imaging ultrasound probe was used to excite the AO signals, and images were formed with no
20 additional signal processing other than that already implemented on clinical machines. The detection of pulsed modulated light was facilitated by the use of a PRC-based interferometer. Deleterious bioeffects of high intensity CW ultrasound are avoided, and using short pulses to excite the AO response enables the utilization of standard imaging technology to yield a true multi-mode imaging capability sensitive to *both* acoustical and
25 optical contrast. These results are presented here derive from *in vitro* experiments on phantoms. To demonstrate the feasibility of this technique for imaging real biological tissue *in vivo*, speckle decorrelation associated with tissue motion has to be overcome, requiring the PRC response time to be short with respect to the speckle decorrelation time *in vivo*. A crystal possessing a response time faster than the BSO crystal used in our setup
30 (approximately 150 ms, requiring some degree of mechanical isolation) must be employed before we can move on to *in vivo* studies.

This work was supported by the Center for Subsurface and Imaging Systems via NSF
ERC award number EEC-9986821)

References

1. V. V. Tuchin, *Handbook of Optical Biomedical Diagnostics* (SPIE, Washington, 2002).
- 5 2. L. V. Wang, "Ultrasound-mediated biophotonic imaging: a review of acousto-optical tomography and photo-acoustic tomography," *Dis Markers* **19**(2-3), 123-138 (2003).
3. L. H. Wang, S. L. Jacques, and X. M. Zhao, "Continuous-Wave Ultrasonic Modulation of Scattered Laser-Light to Image Objects in Turbid Media," *Optics Letters* **20**(6), 629-631 (1995).
- 10 4. M. Kempe, M. Larionov, D. Zaslavsky, and A. Z. Genack, "Acousto-optic tomography with multiply scattered light," *Journal of the Optical Society of America a-Optics Image Science and Vision* **14**(5), 1151-1158 (1997).
5. S. Leveque, A. C. Boccara, M. Lebec, and H. Saint-Jalmes, "Ultrasonic tagging of photon paths in scattering media: parallel speckle modulation processing," *Optics Letters* **24**(3), 181-183 (1999).
- 15 6. A. Lev and B. G. Sfez, "Pulsed ultrasound-modulated light tomography," *Optics Letters* **28**(17), 1549-1551 (2003).
7. B. C. Forget, F. Ramez, M. Atlan, J. Selb, and A. C. Boccara, "High-contrast fast Fourier transform acousto-optical tomography of phantom tissues with a frequency-chirp modulation of the ultrasound," *Applied Optics* **42**(7), 1379-1383 (2003).
- 20 8. S. Leveque-Fort, J. Selb, L. Pottier, and A. C. Boccara, "Towards simultaneous acousto-optical and acoustical imaging in biological tissues," presented at the Photon Migration, Diffuse Spectroscopy, and Optical Coherence Tomography: Imaging and Functional Assessment, 2000.
- 25 9. J. Selb, S. Leveque-Fort, L. Pottier, and A. C. Boccara, "Setup for simultaneous imaging of optical and acoustic contrasts in biological tissues," presented at the Biomedical Optoacoustics II, San Jose, CA, USA, 2001.
- 30 10. T. W. Murray, L. Sui, G. Maguluri, R. A. Roy, A. Nieva, F. Blonigen and C. A. DiMarzio, "Detection of ultrasound modulated photons in diffuse media using the photorefractive effect," *Optics Letters* **in press** (2004).
- 35 11. L. Sui, R. A. Roy, C. A. DiMarzio, and T. W. Murray, "Imaging in diffuse media using pulsed ultrasound-modulated light and the photorefractive effect," *Applied Optics* (submitted).

Figure Captions

Figure 1. Experimental setup combining a PRC based interferometer with the commercial pulsed- ultrasound scanner: VBS- variable beamsplitter, RB- reference beam, SB-
5 signal beam, BE- beam expander, UP- ultrasound probe, L1, 2- lenses, PRC- photorefractive crystal, BP- optical bandpass filter, APD- avalanche photodiode, PA- preamplifier, LP- lowpass filter.

Figure 2. a: B-mode (left) and AO (right) images of a $2 \times 2 \times 8 \text{ mm}^3$ (z,x,y) optical absorber.
10 b: A typical time averaged AO signal as displayed on the oscilloscope for an ultrasound scan line traversing the absorber ($x = 0 \text{ mm}$).

Figure 3. a: B-mode (left) and AO (right) images of two $3 \times 3 \times 8 \text{ mm}^3$ (z,x,y) optical absorbers separated by 3 mm along the z axis. b: A typical time averaged AO
15 signal as displayed on the oscilloscope for a single ultrasound scan line traversing both absorber ($x = 0 \text{ mm}$).

Figure 4. a: B-mode (left) and AO (right) images of two $3 \times 3 \times 8 \text{ mm}^3$ (z,x,y) targets separated by 3 mm along the x axis. The target at $x = -3 \text{ mm}$ is identical to the
20 background medium, whereas the target at $x = +3 \text{ mm}$ is absorbing. b: Typical time averaged AO signals as displayed on the oscilloscope for separate scan lines traversing across each target.

Figure 1

5

10

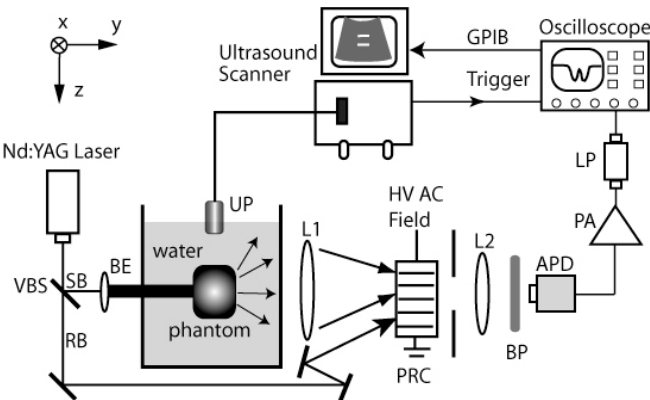


Figure 2

5

10

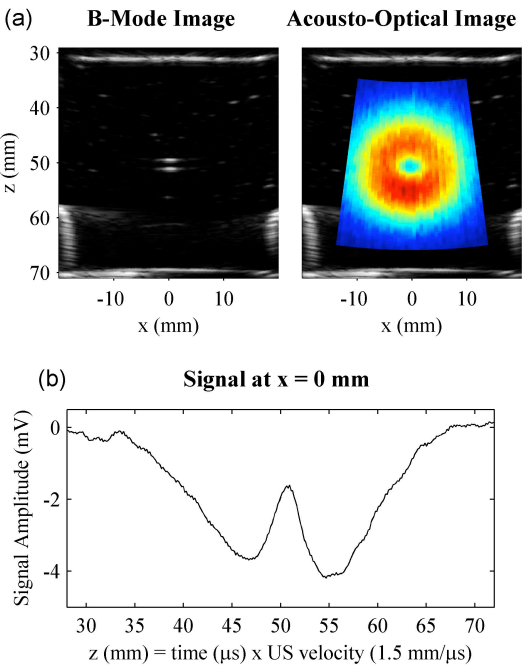


Figure 3

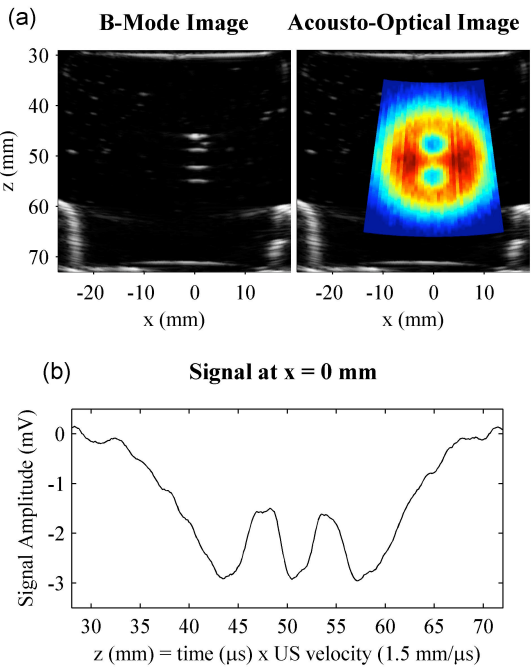


Figure 4

5

